

# The electronic structure of $\text{CuSiO}_3$ – a possible candidate for a new inorganic spin-Peierls compound ?

H. Rosner, S.-L. Drechsler, K. Koepernik, R. Hayn, and H. Eschrig

*Institut für Festkörper- und Werkstofforschung Dresden, P.O. Box 270016, D-01171 Dresden, Germany*

(November 1, 2018)

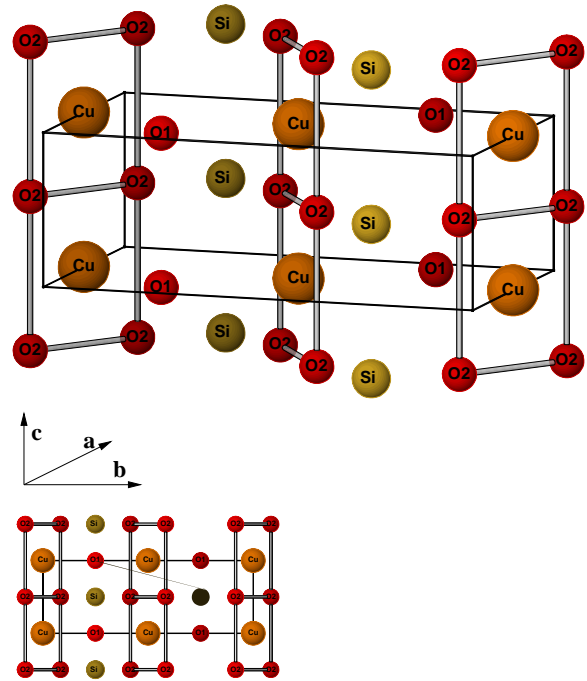
Electronic structure calculations are presented for the well-known  $\text{CuGeO}_3$  and the recently discovered isostructural  $\text{CuSiO}_3$  compounds. The magnitude of the dispersion in chain direction is considerably smaller for  $\text{CuSiO}_3$ , whereas the main interchain couplings are rather similar in both compounds. Starting from extended one-band tight-binding models fitted to the bandstructures, the exchange integrals were estimated for both compounds in terms of a spatially anisotropic Heisenberg model. Remarkable frustrating second neighbor couplings are found both for intra- and inter-chain interactions. A magnetic moment of about  $0.35 \mu_B$  is predicted for  $\text{CuSiO}_3$  in the Néel state.

PACS numbers: 71.15.Mb 71.20.-b 75.30.Et

Low-dimensional spin systems such as chains or ladders are of fundamental interest for contemporary solid state physics due to their peculiar electronic and magnetic properties. During the last years, many related materials have been found within the cuprate family, famous for the high temperature superconductivity. All cuprates contain  $\text{CuO}_4$  plaquettes. In most cases it is energetically favorable to connect these plaquettes by the formation of chains or planes. According to the number ( $n = 1, 2$ ) of oxygen atoms shared by adjacent plaquettes, these compounds can be classified as so-called edge-shared ( $n = 2$ ) or corner-shared ( $n = 1$ ) compounds.

Obviously, the type of sharing affects strongly the physical properties of the compounds under consideration. For example, corner sharing leads to strong antiferromagnetic coupling between neighboring plaquettes compared with the weak inter-chain interactions.<sup>1</sup> As a result, the straight  $\text{CuO}_3$  chain in  $\text{Sr}_2\text{CuO}_3$  is the best known realization of the one-dimensional spin-1/2 Heisenberg model,<sup>2</sup> with an in-chain exchange coupling of about 2200 K, but with a Néel temperature of only 5 K and with an extremely small ordered magnetic moment of about  $0.06 \mu_B$ ,<sup>3</sup> both due to a small residual interchain exchange coupling. Spin-charge separation in the excitation spectra could be observed for  $\text{Sr}_2\text{CuO}_3$  and for the double chain compound  $\text{SrCuO}_2$ .<sup>4</sup>

Somewhat surprisingly, in contrast to the similarity between different corner-shared chain compounds, the magnetic properties in the edge-shared chain family exhibit a remarkable variance. Thus, the edge-shared  $\text{CuO}_2$  plaquettes in  $\text{Li}_2\text{CuO}_2$  order antiferromagnetically with a ferromagnetic arrangement along those chains and with a large ordered moment of  $0.9 \mu_B$ ,<sup>5</sup> whereas the same chain in  $\text{CuGeO}_3$  shows a spin-Peierls transition at low temperatures.<sup>6</sup> Antiferromagnetically ordered chains were observed in  $\text{Cu}_{1-x}\text{Zn}_x\text{GeO}_3$  for small concentrations of Zn impurities.<sup>7</sup> It is noteworthy that, even for the intensively studied  $\text{CuGeO}_3$ , a consensus with respect to the quantitative description of competing or complementary interactions such as the inter-chain coupling, frustration and spin-phonon coupling has not been reached so



properties are the planar edge-shared  $\text{CuO}_2$  chains running along  $\mathbf{c}$ -direction. These chains are very similar to those of  $\text{CuGeO}_3$ . The Cu-O(2) bond length in  $\text{CuSiO}_3$  ( $\text{CuGeO}_3$ ) is 1.941 Å (1.942 Å), the Cu-O(2)-Cu bonding angle is  $94^\circ$  ( $99^\circ$ ).

Thus, the question arises, whether the very recently observed phase transition<sup>11</sup> near 8 K does point to a new inorganic spin-Peierls system or to another ordered state realized at low temperature. To get theoretical insight into possible scenarios, we present here comparative band-structure calculations and tight-binding examinations for  $\text{CuSiO}_3$  and  $\text{CuGeO}_3$ . In this context we note that for the latter compound several (non full-potential) bandstructure calculation have been reported (e.g. in Ref. 12), but to our knowledge the inter-chain interaction has not been analyzed in detail.

The relevant electronic structure of these materials is very sensitive to details of hybridization and charge balance. In order to obtain a realistic and reliable hopping part of a tight binding Hamiltonian, band-structure calculations were performed using the full-potential nonorthogonal local-orbital minimum-basis scheme<sup>13</sup> within the local density approximation (LDA). In the scalar relativistic calculations we used the exchange and correlation potential of Perdew and Zunger.<sup>14</sup> Cu(4s, 4p, 3d), O(2s, 2p, 3d), Ge(3d, 4s, 4p, 4d) and Si(2p, 3s, 3p, 3d) states, respectively, were chosen as minimum basis set. All lower lying states were treated as core states. The inclusion of Ge 3d and Si 2p states in the valence states was necessary to account for non-negligible core-core overlaps. The O and Si 3d as well as the Ge 4d states were taken into account to increase the completeness of the basis set. The spatial extension of the basis orbitals, controlled by a confining potential<sup>15</sup>  $(r/r_0)^4$ , was optimized to minimize the total energy.

The results of the paramagnetic calculation<sup>16</sup> for  $\text{CuSiO}_3$  (see Fig. 2 (a)) and  $\text{CuGeO}_3$  (see Fig. 2 (b); we find similar results as the non full-potential calculation of Ref. 12) show a valence band complex of about 10 eV width with two bands crossing the Fermi level in both cases. These two bands are well separated from the rest of the valence band complex and show mainly Cu 3d and O(2) 2p character in the analysis of the corresponding partial densities of states (not shown). We note that the occupancy of the two O(2) 2p orbitals along and perpendicular to the chain (lying in the plaquette-planes) is rather different, but it is almost identical for the corresponding orbitals in both compounds. Therein, we found only a small admixture of O(1) 2p and Ge 4s and 4p states, respectively, with a total amount of few percent. The examination of the eigenstates of the latter bands at high symmetry points yields an antibonding character typical for cuprates. Here these relatively narrow antibonding bands are half-filled. Therefore, strong correlation effects can be expected which explain the experimentally observed insulating groundstate. Despite almost perfect qualitative one to one correspondence of all valence bands and main peak structures in the den-

sities of states (DOS) (compare right panels in Fig. 2), the most important differences between both compounds

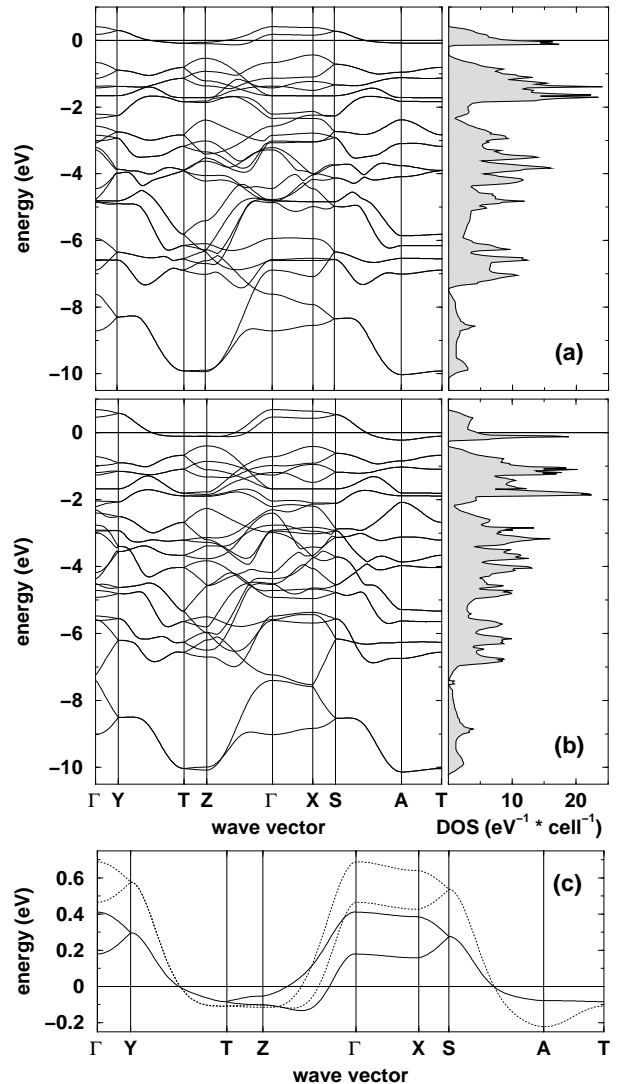


FIG. 2. Band structure and total density of states for  $\text{CuSiO}_3$  (a),  $\text{CuGeO}_3$  (b), and the zoomed antibonding bands (c) ( $\text{CuSiO}_3$  full lines,  $\text{CuGeO}_3$  dashed lines). The Fermi level is at zero energy. The notation of the symmetry points is as follows: Y = (010), T = (011), Z = (001), X = (100), S = (110), A = (111). The chain direction corresponds to Y-T, Z- $\Gamma$  and S-A.

occur for the antibonding bands (shown in detail in Fig. 2(c)). Therefore, we restrict ourselves to the extended tight-binding analysis and the discussion of these antibonding bands.

The dispersion of these bands has been analyzed in terms of nearest neighbor transfer (NN), next nearest neighbor transfer (NNN) and higher neighbor terms in chain direction, but only NN hopping and a diagonal transition term between the  $\text{CuO}_2$ -chains have been considered (see Fig. 3). Then, the corresponding dispersion relation takes the form

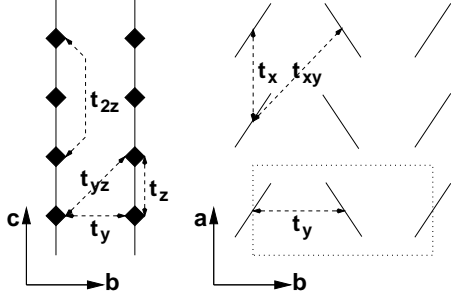


FIG. 3. Schematic chain and stack arrangement of  $\text{CuO}_2$ -plaquettes, respectively, and considered transfer processes within the  $bc$ -plane (left panel) and in the  $ab$ -plane (right panel).

$$E(\vec{k}) = -2 \left( \sum_{m=1,4} t_{mz} \cos(mz) + \cos(x) [t_x + 2t_{xz} \cos(z)] + \cos(y/2) [t_y + 2t_{yz} \cos(z) + 2t_{xy} \cos(x)] \right), \quad (1)$$

where  $x = k_z a$ ,  $y = k_y b$ ,  $z = k_z c$ . Notice that in our effective one-band description the upper band (see Fig. 2(c)) e.g. along  $\Gamma$ -X corresponds to  $k_y = 0$ , whereas the lower one corresponds to  $k_y = 2\pi/b$ . The assignment of the parameters has been achieved by two numerically independent procedures: By straightforward least square fitting of the whole antibonding band in all directions and by using the bandwidths, the slopes and the curvatures at special selected high symmetry points. The latter procedure has the advantage to be less affected by hybridization effects from lower lying bands near the bottom of the antibonding band (being of some relevance near the Z-point in Fig. 2).

	$t_z$	$t_{2z}$	$t_{3z}$	$t_x$	$t_y$	$t_{yz}$
$\text{CuGeO}_3$	-175	-51	-5.5	-20	-34.1	-20.6
$\text{CuSiO}_3$	-88	-31	-4.5	-2.4	-36	-21.2

TABLE I. Transfer integrals  $t_i$  (in meV) of the extended one-band tight-binding model for  $\text{CuGeO}_3$  and  $\text{CuSiO}_3$ . The remaining omitted terms from Eq. (1) were found to be irrelevant.

The results are shown in Tab. I. The errors can be estimated between 1% for the large and 10% for the small parameters from the difference of both mentioned above fitting procedures. The analyzed antibonding bands of both compounds exhibit a rather similar shape except near the Z-points, where the hybridization with lower lying bands produces an additional band-crossing for  $\text{CuGeO}_3$  (see Fig. 2(c)). Recall that the main difference to the corner-shared chains as e.g. in  $\text{Sr}_2\text{CuO}_3$  is a much smaller in-chain NN transfer due to the different geometry.

In spite of the qualitative similarity, the calculated values for the transfer integrals are quite different. The in-chain dispersion is nearly twice as large for  $\text{CuGeO}_3$  in

comparison to  $\text{CuSiO}_3$ . This can be attributed mainly to the larger Cu-O-Cu bond angle in  $\text{CuGeO}_3$  ( $99^\circ$  and  $94^\circ$ , respectively). However, this geometrical effect is somewhat reduced by the different on-site energies of the oxygen orbitals along and perpendicular to the chain (lying in the plaquettes planes). The latter difference is reflected by the larger separation of the corresponding bands at the Z-point in  $\text{CuSiO}_3$  (see Fig. 2).

The inter-chain dispersions in  $b$  direction are comparable. For both compounds, we find also rather significant diagonal hopping terms  $t_{yz}$  which are reflected by different dispersions along the X-S and the T-Z directions. Somewhat surprisingly, we found a sizeable dispersion in  $x$ -direction for  $\text{CuGeO}_3$  but only a very weak one for the  $\text{CuSiO}_3$  counterpart.

From the transfer integrals discussed above, we conclude that both compounds are not so well-defined quasi one-dimensional systems as compared to the corner-shared  $\text{CuO}_3$  chain compounds<sup>1,17</sup>. The inter-chain coupling is rather significant for  $\text{CuGeO}_3$ , and  $\text{CuSiO}_3$  can even be regarded as an anisotropic two-dimensional system. Since increasing inter-chain coupling tends to destabilize the spin-Peierls state<sup>18</sup>, a Néel ordered antiferromagnetic ground state might be expected for  $\text{CuSiO}_3$  in contrast to the spin-Peierls state realized in  $\text{CuGeO}_3$ .

The obtained transfer integrals enables us to estimate the relevant exchange integrals  $J$ . This knowledge is crucial for the derivation and examination of magnetic model Hamiltonians of the spin-1/2 Heisenberg type frequently used in the literature:

$$H_{spin} = \sum_{ij} J_{ij} \vec{S}_i \vec{S}_j. \quad (2)$$

In general, the total exchange  $J$  can be divided into an antiferromagnetic and a ferromagnetic contribution  $J = J^{AFM} + J^{FM}$ . In the strongly correlated limit, valid for typical cuprates, the former can be calculated in terms of the one-band extended Hubbard model  $J_{ij}^{AFM} = 4t_{ij}^2 / (U - V_{ij})$ . The indices  $i$  and  $j$  correspond to nearest and next nearest neighbors,  $U$  is the on-site Coulomb repulsion and  $V_{ij}$  is the inter-site Coulomb interaction. From experimental data<sup>19</sup> mapped from the standard  $pd$ -model onto the one-band description, one estimates  $U - V \sim 4.2$  eV. For the sake of simplicity, we neglect the difference in the quantity  $U - V$  in the compounds. The calculated values for the exchange integrals are given in Tab. II.

	$J_1^{AFM}$	$J_1$	$J_2$	$J_x$	$J_y$	$J_{yz}$	$\mu_{th}$	$\mu_{exp}$
$\text{CuGeO}_3$	29	15	2.5	0.4	1.11	0.4	0.17	0.21
$\text{CuSiO}_3$	7.4	3.8	0.9	0.006	1.25	0.43	0.35	unknown

TABLE II. Exchange parameters  $J_i$  (in meV) for  $\text{CuGeO}_3$  and  $\text{CuSiO}_3$ , and local magnetic moments (in  $\mu_B$ ) in the Néel state derived from them (see text). The experimental value  $\mu_{ex}$  is an average over various studies mentioned in the text.

The value of the NN exchange integral  $J_1^{AFM} \sim 30$  meV in  $\text{CuGeO}_3$  exceeds the experimental values of about 11 meV from inelastic neutron scattering data<sup>20</sup>, about 14 meV from magnetic susceptibility<sup>21</sup> and about 22 meV from Raman scattering<sup>22</sup>. This points to a significant ferromagnetic contribution due to the Goodenough-Kanamori-Anderson-type interaction<sup>23</sup>. In the following, we shall adopt 15 meV for the resulting total exchange coupling  $J_1$  as a representative value, suggested by the average of the above mentioned experimental data. Owing to the lack of experimental data we assume the same ratio  $J_1/J_1^{AFM}$  in  $\text{CuSiO}_3$  as in  $\text{CuGeO}_3$ , suggested by the quite similar O(2)  $2p$  orbital occupancies mentioned above. For the latter compound, we note the reasonable agreement with the available experimental data and most of our calculated antiferromagnetic values for the remaining exchange parameters. Hence, further possible ferromagnetic contributions seem to be less relevant and are neglected in the following considerations.

Further simplification can be obtained mapping  $J_1$  and the frustrated NN term  $J_2$  onto an effective intra-chain coupling  $J_{\parallel} = J_1 - 1.12J_2$ .<sup>24</sup> The calculated values for  $J_{\parallel}$  are 12.2 meV for  $\text{CuGeO}_3$  and 2.8 meV for  $\text{CuSiO}_3$ , respectively. The latter value is close to the value of 2 meV reported by Baenitz *et al.* from a one-dimensional fit of magnetic susceptibility data.<sup>11</sup> We find also a considerable inter-chain frustration  $J_{yz} = \beta J_y$  with  $\beta=0.36$  (0.34) for the Ge- (Si-) compound. This is in good agreement with the suggestions of Uhrig<sup>8</sup>  $\beta \approx 0.5$  for  $\text{CuGeO}_3$ .

Transferring the above mentioned idea to map frustrating terms onto one effective coupling,<sup>24</sup> we adopt  $J_{\perp} = J_y - 2J_{yz}$  for the effective inter-chain exchange parameters in  $b$ -direction. The factor of two is introduced to account approximately the twice as large number of second neighbors. The effective anisotropy ratio  $R = J_{\perp}/J_{\parallel}$  measures approximately the magnitude of quantum fluctuations. In the crossover region between one and two dimensions, quantum fluctuations do strongly affect the magnitude of the staggered magnetization  $m$  and the local Cu moment  $\mu = g_L n_d m$  at  $T = 0$  for a Néel ground state, where  $g_L=2.06$  to  $2.26$ <sup>25</sup> denotes the (anisotropic) Landé-factor (tensor) for  $\text{Cu}^{2+}$  in  $\text{CuGeO}_3$  and  $n_d \approx 0.8$  is the hole occupation number of the related Cu  $3d$  plaquette orbital. Using the expression

$$m = 0.39\sqrt{R}(1 + 0.095R) \ln^{1/3}(1.3/R), \quad (3)$$

taken from Ref. 26, we arrive at  $0.17\mu_B$  in reasonable agreement<sup>27</sup> with the neutron data  $0.22 \pm 0.02$ <sup>28</sup> and  $0.2$ <sup>29</sup> for the disorder induced Néel state achieved below 4.5K in Zn-doped  $\text{CuGeO}_3$ . The same approach predicts a significantly larger value of about  $0.35\mu_B$  for  $\text{CuSiO}_3$  realized in a possible Néel state.

To summarize, our LDA-FPLO calculation reveals valuable insight into the relevant couplings of  $\text{CuGeO}_3$  and  $\text{CuSiO}_3$ . We can classify  $\text{CuGeO}_3$  as a quasi one-dimensional compound with significant inter-chain interaction, whereas  $\text{CuSiO}_3$  is closer to an anisotropic two-dimensional compound. The significantly reduced energy

scale of the in-chain exchange interactions and the large inter-chain interaction in  $\text{CuSiO}_3$  are less favorable for a spin-Peierls state than for a Néel order. However, due to the large frustrations other states such as a spin-Peierls state cannot be excluded. Further investigations are required to elucidate the unknown ground state.

We acknowledge fruitful discussions with M. Baenitz, C. Geibel, W. Pickett and G. Uhrig. This work was supported by individual grants of the DAAD (H.R.) and the DFG (S.D.).

- 
- <sup>1</sup> H. Rosner *et al.*, Phys. Rev. B **56**, 3402 (1997).
  - <sup>2</sup> A. Tsvelik, *Quantum Field Theorie in Condensed Matter* (Cambridge University Press, Cambridge, 1995).
  - <sup>3</sup> K. M. Kojima *et al.*, Phys. Rev. Lett. **78**, 1787 (1997).
  - <sup>4</sup> C. Kim *et al.*, Phys. Rev. Lett. **77**, 4054 (1996).
  - <sup>5</sup> F. Sapiña *et al.*, Solid State Comm. **74**, 779 (1990).
  - <sup>6</sup> M. Hase *et al.*, Phys. Rev. Lett. **70**, 3651 (1993).
  - <sup>7</sup> M. Hase *et al.*, Phys. Rev. Lett. **71**, 4059 (1993).
  - <sup>8</sup> G. Uhrig, Phys. Rev. Lett. **79**, 163 (1997).
  - <sup>9</sup> G. Bouzerar *et al.*, Phys. Rev. B **60**, 15278 (1999).
  - <sup>10</sup> H. H. Otto *et al.*, Z. f. Kristallogr. **214**, 558 (1999).
  - <sup>11</sup> M. Baenitz, to be published.
  - <sup>12</sup> L. F. Mattheiss, Phys. Rev. B **49**, 14050 (1994).
  - <sup>13</sup> K. Koepnik and H. Eschrig, Phys. Rev. B **59**, 1743 (1999).
  - <sup>14</sup> J. P. Perdew and A. Zunger, Phys. Rev. B **23**, 5048 (1981).
  - <sup>15</sup> H. Eschrig, *Optimized LCAO Method and the Electronic Structure of Extended Systems* (Springer, Berlin, 1989).
  - <sup>16</sup> For the tight-binding analysis, the paramagnetic solutions are sufficient. Magnetic LSDA solutions were also found for both compounds showing insulating behavior, but due to the insufficient treatment of correlation in the LSDA the calculated gap is much too small.
  - <sup>17</sup> H. Rosner *et al.*, Physica B **259–261**, 1001 (1999).
  - <sup>18</sup> S. Inagaki *et al.*, J. Phys. Soc. Jpn. **52**, 3620 (1983).
  - <sup>19</sup> F. Parmigiani *et al.*, Phys. Rev. B **55**, 1459 (1996).
  - <sup>20</sup> L. P. Regnault *et al.*, Phys. Rev. B **53**, 5579 (1996).
  - <sup>21</sup> K. Fabricius *et al.*, Phys. Rev. B **57**, 1102 (1998).
  - <sup>22</sup> H. Kuroe *et al.*, Phys. Rev. B **55**, 409 (1997).
  - <sup>23</sup> P. W. Anderson, Phys. Rev. **115**, 2 (1959).
  - <sup>24</sup> A. Fledderjohann *et al.*, Europhys. Lett. **37**, 189 (1997).
  - <sup>25</sup> M. Honda *et al.*, J. Phys. Soc. Jpn. **65**, 691 (1996).
  - <sup>26</sup> A. W. Sandvik, Phys. Rev. Lett. **83**, 3069 (1999).
  - <sup>27</sup> The estimated moment should be regarded as a lower bound due to the neglected weak interaction in  $x$ -direction which reduces further the quantum fluctuations. Due to the Mermin-Wagner-theorem, this interaction is crucial for the finite Néel temperature not considered here.
  - <sup>28</sup> M. Hase *et al.*, J. Phys. Soc. Jpn. **65**, 273 (1996).
  - <sup>29</sup> Y. Sasago *et al.*, Phys. Rev. B **54**, 6835 (1996).